Available online at www.sciencedirect.com

SciVerse ScienceDirect

Geochimica et Cosmochimica Acta 75 (2011) 7472–7485

Geochimica et Cosmochimica Acta

www.elsevier.com/locate/gca

Production of *n*-alkyl lipids in living plants and implications for the geologic past

Aaron F. Diefendorf [a,*], Katherine H. Freeman [b], Scott L. Wing [c], Heather V. Graham [b]

[a] *Department of Geology, PO Box 210013, University of Cincinnati, Cincinnati, OH 45221-0013, USA*
[b] *Department of Geosciences, Pennsylvania State University, University Park, PA 16802, USA*
[c] *Department of Paleobiology, NHB121, P.O. Box 37012, Smithsonian Institution, Washington, DC 20013, USA*

Received 8 March 2011; accepted in revised form 14 September 2011

Abstract

Leaf waxes (i.e., *n*-alkyl lipids or *n*-alkanes) are land-plant biomarkers widely used to reconstruct changes in climate and the carbon isotopic composition of the atmosphere. There is little information available, however, on how the production of leaf waxes by different kinds of plants might influence the abundance and isotopic composition of *n*-alkanes in sedimentary archives. This lack of information increases uncertainty in interpreting *n*-alkyl lipid abundance and $\delta^{13}C$ signals in ancient settings. We provide here *n*-alkyl abundance distributions and carbon isotope fractionation data for deciduous and evergreen angiosperm and gymnosperm leaves from 46 tree species, representing 24 families. *n*-Alkane abundances are significantly higher in angiosperms than gymnosperms; many of the gymnosperm species investigated did not produce any *n*-alkanes. On average, deciduous angiosperms produce 200 times more *n*-alkanes than deciduous gymnosperms. Although differences between angiosperms and gymnosperms dominate the variance in *n*-alkane abundance, leaf life-span is also important, with higher *n*-alkane abundances in longer-lived leaves. *n*-Alkanol abundances covary with *n*-alkanes, but *n*-alkanoic acids have similar abundances across all plant groups. Isotopic fractionation between leaf tissue and individual alkanes (ε_{lipid}) varies by as much as 10‰ among different chain lengths. Overall, ε_{lipid} values are slightly lower (−4.5‰) for angiosperm than for gymnosperm (−2.5‰) *n*-alkanes. Angiosperms commonly express slightly higher Δ_{leaf} (photosynthetic discrimination) relative to gymnosperms under similar growth conditions. As a result, angiosperm *n*-alkanes are expected to be generally 3–5‰ more depleted in ^{13}C relative to gymnosperm alkanes for the same locality. Differences in *n*-alkane production indicate the biomarker record will largely (but not exclusively) reflect angiosperms if both groups were present, and also that evergreen plants will likely be overrepresented compared with deciduous ones. We apply our modern lipid abundance patterns and ε_{lipid} results to constrain the magnitude of the carbon isotope excursion (CIE) at the onset of the Paleocene–Eocene Thermal Maximum (55.8 Ma). When Bighorn Basin (WY) sediment *n*-alkanes are interpreted in context of floral changes and modern *n*-alkane production estimates for angiosperms and gymnosperms, the CIE is greater in magnitude (−5.6‰) by ~1‰ compared to previous estimates that do not take into account *n*-alkane production.

1. INTRODUCTION

The use of biomarkers, molecular fossils specific to a biological source, has become routine to reconstruct past climates from marine (Freeman and Hayes, 1992) and terrestrial sediments (e.g., Pancost and Boot, 2004). Increasingly, biomarkers from plants are used to track terrestrial climates and ecosystems in the geologic past to further our understanding of ancient environmental and climatic change (Bird et al., 1995; Huang et al., 1995; Logan et al., 1995; Freeman and Colarusso, 2001; Schouten et al., 2007). Terrestrial biomarker studies have primarily

* Corresponding author.
E-mail address: aaron.diefendorf@uc.edu (A.F. Diefendorf).

0016-7037/$ - see front matter © 2011 Elsevier Ltd. All rights reserved.
doi:10.1016/j.gca.2011.09.028

focused on leaf waxes (Fig. 1) such as *n*-alkanes (I), *n*-alkanols (II), and *n*-alkanoic acids (III) with the majority focusing on *n*-alkanes due to their high preservation potential (e.g., Cranwell, 1981). Compound-specific analyses of both carbon and hydrogen isotopes complement studies of terrestrial biomarkers and are increasingly important to understanding the response of carbon and water cycles to past climate perturbations. Molecular carbon isotope ($\delta^{13}C$) signatures are less influenced by diagenesis, differential preservation of compound classes, and changes in the sources of organic matter that otherwise complicate interpretations of bulk $\delta^{13}C$ values (e.g., Pancost and Boot, 2004).

Waxes are found in various locations within the leaf cuticle. The function of this cuticle is to protect and isolate leaf tissues from the atmosphere. The cuticle is divided into several layers, including the cuticle proper, an epicuticular wax layer, and an epicuticular wax crystal layer (Eglinton et al., 1962; Eglinton and Hamilton, 1967); each with discrete chemical compositions (Jetter et al., 2000). Within the cuticle is a matrix of cutin, a polyester biopolymer made of hydroxy fatty acids and waxes (Eglinton et al., 1962; Eglinton and Hamilton, 1967; Baker, 1982; Holloway and Williams, 1982). The epicuticular wax layer contains *n*-alkanes and free and ester-bound long-chain *n*-alkyl wax lipids (Fig. 1, IV) including fatty acids (*n*-alkanoic acids) and alcohols (*n*-alkanols). These leaf waxes have diverse functions (see review, Koch and Ensikat, 2008), including inhibiting the loss of water from the leaf (e.g., Riederer and Schreiber, 2001), limiting the transport of water (and thus dissolved chemicals) into the leaf (Bargel et al., 2006), keeping the leaf surface clean, increasing disease resistance (Muller and Riederer, 2005), and providing ultraviolet light protection to leaf tissue (Bargel et al., 2006).

Leaf wax composition and abundance can vary with ontogeny (Lockheart et al., 1997; Jetter and Schaffer, 2001; Sachse et al., 2009), environmental variables and stresses (Jetter and Schaffer, 2001; Dodd and Poveda, 2003; Shepherd and Griffiths, 2006), and among plant families (Eglinton and Hamilton, 1967; Baker, 1982; Piasentier et al., 2000; Dodd and Poveda, 2003). Most alkane abundance data are reported relative to the most abundant component, and to our knowledge, no one has quantified variation in *n*-alkyl lipid concentrations among plants at the same site that differ in their leaf phenology and phylogenetic group.

Long-chain *n*-alkyl lipids are biosynthesized in the acetogenic pathway from acetyl coenzyme-A (acetyl CoA) monomers to produce *n*-alkanoic acids. The *n*-alkanoic acids are converted to *n*-alkanes via enzymatic decarboxylation or to *n*-alkanols through reduction (Eglinton and Hamilton, 1967; Kolattukudy et al., 1976; Kolattukudy, 1996; Kunst and Samuels, 2003; Chikaraishi et al., 2004). The underlying mechanisms for moving *n*-alkyl lipids from the epidermal cells, where they are formed, to the epicuticular layer is uncertain (Kunst and Samuels, 2003).

Carbon isotope fractionation between atmospheric CO_2 and leaf carbon (Δ_{leaf}) is well characterized for different photosynthetic pathways (e.g., Deines, 1980; Farquhar et al., 1989). Δ_{leaf} is also correlated with different plant functional types (PFTs; deciduous or evergreen, gymnosperm or angiosperm) and environmental factors, particularly water (Diefendorf et al., 2010). These relationships can thus be used to predict carbon isotope fractionation and $\delta^{13}C$ values of biomarkers in the geologic past from independent estimates of plant community and climate (Diefendorf et al., 2010). However, when authors interpret sedimentary biomarkers, they generally assume that: (1) all plants produce equal amounts of *n*-alkanes and, (2) carbon isotope fractionation during lipid biosynthesis does not vary with PFT or phylogenetic position. These assumptions are known to be incorrect, however, since both *n*-alkane production and biosynthetic fractionation (ε_{lipid}) vary among plant types (Lockheart et al., 1997).

We investigated leaf *n*-alkyl lipid abundances, chain length distributions and their carbon isotopic abundances for 46 tree species, representing 24 families and including deciduous and evergreen angiosperms and gymnosperms. We attempted to minimize extrinsic environmental factors for the largest portion of the dataset by sampling trees grown in a botanical garden (Penn State University) where climate, light, and growing conditions are similar (see Primack and Miller-Rushing, 2009), and we sampled within a short time period to minimize ontogenetic effects. We also included species from a dry site in Wyoming and from a wet tropical site in Panama to increase diversity in species and plant functional type. The objectives of this study were to determine *n*-alkyl lipid abundance patterns and ε_{lipid} for different PFTs. Using these data, we aim to determine the potential for *n*-alkane records to be biased and to understand how these biases influence interpretation of $\delta^{13}C$ records from *n*-alkanes in ancient sediments.

2. METHODS

2.1. Leaf samples locations and preparation

Fresh leaf samples were collected from mature trees (Table 1) at the Pennsylvania State University (University Park, PA, USA) during August and September of 2009

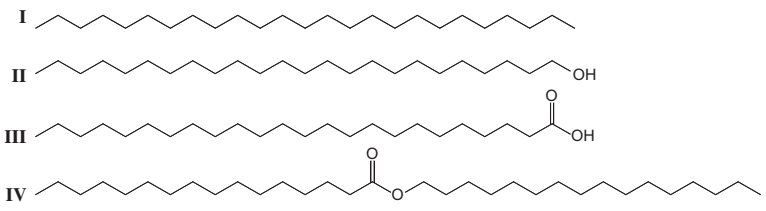

Fig. 1. *n*-Alkyl lipid structures commonly found in plants including *n*-alkanes (I, *n*-C_{25} shown), *n*-alkanols (II, *n*-C_{24} shown), *n*-alkanoic acids (III, *n*-C_{24} shown), and wax esters (IV).

and from two locations within the Bighorn Basin (WY, USA). Additional samples were collected from the Bosque Protector San Lorenzo in Panama during January and February of 2010. Leaves or needles (~10 g) were cut from multiple branches on each individual on the fully exposed sun side of the tree at 2–3 m above ground in North American samples and 30–35 m in Panamanian samples. We sampled evergreen conifer needles that developed during the sampling year. Total number of leaves averaged ~20 for angiosperms and >40 for gymnosperms. Leaves were rinsed with distilled water, cut into <2 cm pieces, and freeze-dried.

2.2. Lipid extraction and fractionation

Powdered leaves (~200 mg) were extracted using an accelerated solvent extractor (Dionex ASE 200) with

Table 1
Location, plant functional types, family, and species sampled.

Location[a]	PFT[b]	Family	Species
PA	DA	Altingiaceae	*Liquidambar styraciflua*
PA	DA	Betulaceae	*Betula papyrifera*
PA	DA	Betulaceae	*Carpinus betulus*
PA	DA	Betulaceae	*Carpinus betulus* 'Fastigiata'
PA	DA	Cannabaceae	*Celtis occidentalis*
PA	DA	Cercidiphyllaceae	*Cercidiphyllum japonicum*
PA	DA	Cornaceae	*Cornus florida*
PA	DA	Cornaceae	*Nyssia sylvatica*
PA	DA	Fabaceae	*Gleditsia triacanthos* 'Inermis'
PA	DA	Fagaceae	*Fagus grandifolia*
PA	DA	Fagaceae	*Quercus alba*
PA	DA	Hamamelidaceae	*Hamamelis virginiana*
PA	DA	Juglandaceae	*Carya ovata*
PA	DA	Juglandaceae	*Pterocarya fraxinifolia*
PA	DA	Lauraceae	*Sassafras albidum*
PA	DA	Magnoliaceae	*Magnolia virginiana*
PA	DA	Malvaceae	*Tilia cordata*
PA	DA	Platanaceae	*Platanus occidentalis*
PA	DA	Salicaceae	*Populus deltoides*
PA	DA	Salicaceae	*Salix babylonica*
PA	DA	Sapindaceae	*Acer rubrum*
PA	DA	Sapindaceae	*Aesculus glabra*
PA	DA	Sapindaceae	*Koelreuteria paniculata*
PA	DA	Ulmaceae	*Ulmus americana*
PA	DA	Ulmaceae	*Zelkova serrata*
PA	DG	Cupressaceae	*Metasequoia glyptostroboides*
PA	DG	Cupressaceae	*Taxodium distichum*
PA	DG	Ginkgoaceae	*Ginkgo biloba*
PA	DG	Pinaceae	*Larix decidua*
PA	EA	Aquifoliaceae	*Ilex opaca*
PA	EA	Ericaceae	*Kalmia latifolia*
PA	EA	Ericaceae	*Rhododendron maximum*
PA	EG	Cupressaceae	*Cryptomeria japonica*
PA	EG	Cupressaceae	*Thuja occidentalis*
PA	EG	Pinaceae	*Abies concolor*
PA	EG	Pinaceae	*Cedrus atlantica* 'Glauca'
PA	EG	Pinaceae	*Picea abies*
PA	EG	Pinaceae	*Pinus flexilis*
PA	EG	Pinaceae	*Pinus sylvestris*
PA	EG	Pinaceae	*Pseudotsuga menziesii*
WY-CF	DA	Salicaceae	*Populus angustifolia*
WY-CF	DA	Salicaceae	*Salix alba*
WY-CG	EG	Cupressaceae	*Juniperus osteosperma*
WY-CG	EG	Pinaceae	*Pinus contorta*
WY-CG	EG	Pinaceae	*Pinus flexilis*
Panama	EA	Apocynaceae	*Aspidosperma* sp.
Panama	EA	Clusiaceae	*Calophyllum* sp.
Panama	EA	Sapotaceae	*Manilkara* sp.

[a] PA, Penn State University (40.7956°N 77.8639°W, 360 m); WY-CF, Wyoming Cabin Fork (43.98185°N 107.67353°W 1480 m); WY-CG, Wyoming Castle Gardens (42.931057°N 107.617792°W, 1870 m); Panama (9.2833°N 79.9750°W, 130 m).
[b] PFT, plant functional type: A, angiosperm; D, deciduous; E, evergreen; G, gymnosperm.

dichloromethane (DCM)/methanol (MeOH) (65:35, v/v) over three extraction cycles at ~6.9 MPa bar (1100 psi) and 100 °C. The total lipid extract (TLE) was concentrated with nitrogen in a Zymark TurboVap LV. The TLE was base saponified, to cleave ester bound fatty acids and alcohols, with 3 ml of 0.5 N KOH MeOH/H_2O (3:1, v/v) for 2 h at 75 °C. After cooling, ~2.5 ml of NaCl in water (5%, w/w) was added to the saponified lipid extract (SLE) and acidified with 6 N HCl to a pH of ~1. The acidic solution was extracted with hexanes/DCM (4:1, v/v), neutralized with $NaHCO_3/H_2O$ (5%, w/w), followed by water removal over Na_2SO_4.

The SLE was separated into four polarity fractions with 0.5 g of aminopropyl-bonded silica gel in 6 ml glass solid phase extraction columns (see Sessions, 2006) under pressure (~13 kPa). Hydrocarbons were eluted with 4 ml hexanes (100%) in the first fraction, ketones were eluted with 8 ml hexanes/DCM (6:1, v/v) in the second fraction, alcohols were eluted with 8 ml of DCM/acetone (9:1, v/v) in the third fraction, and acids were eluted in a fourth fraction with 8 ml of DCM/85% formic acid (49:1 v/v). All fractions were gently dried with nitrogen. Prior to analyses, aliquots of alcohol and acid fractions were converted to trimethylsilyl (TMS) derivatives by reaction with 50 μl of *N,O*-bis(trimethylsilyl)trifluoroacetamide (BSTFA) and 50 μl of pyridine at 70 °C for 20 min. All fractions were analyzed by gas chromatography (GC), GC/mass spectrometry (GC/MS), and isotope ratio monitoring GC/MS (irm-GCMS).

2.3. Identification and quantification

Lipids were identified in each fraction by GC–MS using a Hewlett-Packard (HP) 6890 GC connected to a HP 5973 quadropole MS with electron-impact ionization and with a split/splitless injector operated in pulsed splitless mode at 320 °C. A fused silica capillary column (Agilent J&W DB-5; 30 m, 0.25 mm) coated with (5%-phenyl)-methylpolysiloxane (25-μm film thickness) was used with helium as the carrier gas. For the hydrocarbon fraction, the column flow rate was 2.0 ml/min and the oven program started with an initial temperature of 60 °C for 1 min, followed by a ramp to 320 °C at 6 °C/min, and a final hold of 20 min. For the derivatized alcohol and acid fractions, the column flow rate was 1.5 ml/min and the oven program started with an initial temperature of 60 °C for 1 min, followed by a ramp to 140 °C at 15 °C/min, then a ramp of 4 °C to 320 °C, and then a final hold of 20 min. The MS was operated with a scanning mass range of *m/z* 50–700 at 3 scans per second and an ionization energy of 70 eV. Compounds were identified using authentic standards, NIST 98 spectral library, fragmentation patterns, and retention times.

Prior to quantification of lipids, a known aliquot of each fraction was spiked with internal standards hexadecane and 1,1′-binaphthyl in the hydrocarbon fraction, and with phthalic acid and 2-dodecanol in the alcohol and acid fractions. Compounds were quantified on a HP 5890 GC with a flame ionization detector (FID) using GC conditions as described above. Compound peak areas were normalized to those for 1,1′-binaphthyl or phthalic acid and converted to mass quantities using response curves for ~30 surrogate standard compounds analyzed in concentrations ranging from 0.1 to 120 μg/ml. Accuracy and precision of measurements are 5.5% (1σ, $n = 56$) and 5.7% (1σ, $n = 56$), respectively, and were determined by treating additional analyses of external standards as unknowns. Lipid concentrations were normalized to the mass of dry leaf material extracted.

2.4. Compound-specific carbon isotopes analyses

n-Alkyl lipids were separated on a Varian model 3400 GC equipped with a split/splitless injector operated in splitless mode with a fused silica column (Agilent J&W DB-5; 30 m, 0.32 mm, 0.25 μm). GC conditions were as above. Following GC separation, compounds were combusted over nickel and platinum wire with O_2 in He (1%, v/v) at 1000 °C with the resulting CO_2 monitored using a Finnegan Mat 252 and isotopic abundances determined relative to a reference gas calibrated with Mix A (*n*-C_{16} to *n*-C_{30}; Arndt Schimmelmann, Indiana University). Carbon isotope values of samples (SA) are reported in delta notation relative to the standard Vienna Pee Dee Belemnite (VPDB) as $\delta^{13}C = [(^{13}R_{SA}/^{13}R_{VPDB}) - 1]$ where $^{13}R = {}^{13}C/{}^{12}C$. Within run precision (degree of reproducibility) and accuracy (degree of closeness to the true value) of all samples was determined with co-injected internal standards (*n*-C_{38} and *n*-C_{41} alkanes) and is 0.16‰ (1σ, $n = 103$) and −0.02‰ ($n = 103$), respectively.

2.5. Bulk carbon isotope analyses

$\delta^{13}C$ of leaves ($\delta^{13}C_{leaf}$) and weight percent total organic carbon (TOC) were determined via continuous flow (He; 120 mL/min) on a Costech elemental analyzer (EA) by oxidation at 1020 °C over chromium (III) oxide and silvered cobalt (II, III) oxide followed by reduction over elemental copper at 650 °C. CO_2 was subsequently passed through a water trap and then a 5 Å molecular sieve GC at 50 °C to separate N_2 from CO_2. CO_2 was diluted with helium in a Conflo III interface/open split prior to analysis. $\delta^{13}C$ values were measured on a Thermo Finnegan Delta Plus XP irmMS. Measured $\delta^{13}C$ values were corrected for sample size dependency and then normalized to the VPDB scale with a two-point calibration (Coplen et al., 2006). Error was determined by analyzing independent standards across all EA runs. Accuracy is ±0.02‰ ($n = 54$) and precision is ±0.02‰ ($n = 88$; 1σ).

2.6. Leaf traits

To compare *n*-alkyl lipid results with leaf traits, we compiled leaf mass per area (LMA; Roderick and Cochrane, 2002) from the GLOPNET database (Wright et al., 2004). A total of 28 species were in common between datasets. Panama trees are not included in this comparison because species level identification is not available. We further limited LMA data from the GLOPNET database to temperate forests and woodlands to minimize environmental differences in LMA data. LMA data from the GLOPNET database is provided in EA-1.

3. RESULTS

3.1. Leaf *n*-alkyl lipid abundance and chain length distributions

The total concentration of *n*-alkanes for each species is provided in Fig. 2 and in electronic annex EA-1. There are fewer Wyoming and Panama specimens ($n = 5$ and 3, respectively; Table 1) relative to Pennsylvania specimens, but they provide species and plant functional types that are not otherwise represented. *n*-Alkanes were detected in all angiosperms species but in only 7 of 15 gymnosperm species. The angiosperms also have higher total *n*-alkane abundances than all gymnosperms except *Cryptomeria japonica* and *Juniperus osteosperma*. The variation in total *n*-alkane abundances is high for angiosperms and does not appear to correlate with family (Fig. 2). For example, the *n*-alkane abundances vary greatly among Betulaceae, with total *n*-alkanes ranging from <50 μg/g dry leaf in *Carpinus betulus* to 1300 μg/g dry leaf in *Betula papyrifera*. Among gymnosperm families, Cupressaceae have higher total *n*-alkane abundances than Pinaceae, and no *n*-alkanes were detected in Ginkgoaceae.

The *n*-alkane distributions by plant functional type (PFT) are shown in Table 2 and Fig. 3. The *n*-alkane chain lengths range from *n*-C_{23} to *n*-C_{35} in both gymnosperms and angiosperms and the dominant chain lengths are different among PFTs and taxonomic groups. *n*-Alkane abundances are highest in the evergreen angiosperms (EA) with a maximum of 405 μg/g dry leaf of *n*-C_{31}, followed by the deciduous angiosperms (DA) with a maximum of 162 μg/g dry leaf of *n*-C_{29}. The evergreen gymnosperms (EG) have a higher chain-length maximum at *n*-C_{33} but with much lower abundances (31 μg/g dry leaf). Deciduous gymnosperms (DG) have the lowest abundances, with a maximum of 2 μg/g dry leaf of *n*-C_{29}. The angiosperms have approximately two orders of magnitude more odd *n*-alkanes between *n*-C_{25} to *n*-C_{33} than the gymnosperms (Table 2). The abundance of *n*-C_{35} is not statistically different between angiosperms and gymnosperms, reflecting both lower abundances of *n*-C_{35} in angiosperms, and greater amounts of long-chain *n*-alkanes in *Juniperus* and *Cryptomeria*. Total *n*-alkane abundances are similar between EA species collected in Pennsylvania and Panama (Fig. 2), but Panamanian EAs have a higher proportion of longer chain length *n*-alkanes (e.g., *n*-C_{35}).

The *n*-alkanol abundances (Fig. 3 and EA-1) are characterized by even-chain lengths ranging from *n*-C_{22} to *n*-C_{34}. The highest abundances are found in the DAs with a maximum at *n*-C_{26} (369 μg/g dry leaf). The *n*-alkanoic acids are most abundant in DAs and the EGs, which have a chain length maximum at *n*-C_{22}, with 143 and 204 μg/g dry leaf, respectively. Overall, *n*-alkanoic acid abundances (Fig. 3 and EA-1) are generally similar between PFTs in contrast to the *n*-alkanes and the *n*-alkanols that vary with PFT. Total *n*-alkyl lipid abundances including the *n*-alkanes (>*n*-C_{23}), *n*-alkanols (>*n*-C_{22}), and *n*-alkanoic acids (>*n*-C_{22}) are highest in the DAs compared to other PFTs (Fig. 4). Neither total *n*-alkyl lipid nor total *n*-alkane abundances are correlated with LMA (Fig. 5a and b).

To characterize average *n*-alkane chain lengths (ACL) between different PFTs and plant families, we have calculated ACL using the equation of Eglinton and Hamilton (1967):

$$\mathrm{ACL} = \frac{(25n\text{-}C_{25} + 27n\text{-}C_{27} + 29n\text{-}C_{29} + 31n\text{-}C_{31} + 33n\text{-}C_{33} + 35n\text{-}C_{35})}{(n\text{-}C_{25} + n\text{-}C_{27} + n\text{-}C_{29} + n\text{-}C_{31} + n\text{-}C_{33} + n\text{-}C_{35})} \quad (1)$$

where *n*-alkane abundances are converted to respective chain length numbers (Fig. 6 and EA-1). ACL varies substantially between PFTs and between plant families and species. The highest ACL values are for the EGs, however their ACL range is quite large, from 26 to 34, and has a bimodal distribution by family with the Pinaceae averaging 27 and the Cupressaceae averaging 32. Values for the DAs span from 27 to over 32. However, means between PFTs and phylogenetic groups are not statistically different (Wilcoxon test).

We found small but variable amounts of *n*-alkanes with even-chain lengths in many of the plant samples. We calculate the carbon preference indices (CPI) for *n*-alkanes using the equation of Bray and Evans (1961):

$$\mathrm{CPI} = 0.5\left[\frac{(n\text{-}C_{25} + n\text{-}C_{27} + n\text{-}C_{29} + n\text{-}C_{31} + n\text{-}C_{33})}{(n\text{-}C_{26} + n\text{-}C_{28} + n\text{-}C_{30} + n\text{-}C_{32} + n\text{-}C_{34})} + \frac{(n\text{-}C_{25} + n\text{-}C_{27} + n\text{-}C_{29} + n\text{-}C_{31} + n\text{-}C_{33})}{(n\text{-}C_{24} + n\text{-}C_{26} + n\text{-}C_{28} + n\text{-}C_{30} + n\text{-}C_{32})}\right] \quad (2)$$

where values >1 are characterized by higher odd-chain *n*-alkane abundances than even-chain abundances. Values are shown in Fig. 7 and EA-1. CPI values for species that contain *n*-alkanes vary between 1.6 and 82.1, indicating that all species have a strong odd-chain preference. Generally DAs have the highest CPI values and DGs have the lowest.

3.2. *n*-Alkane lipid biosynthetic fractionation

Carbon isotope values of *n*-alkanes and bulk leaf tissues (reported in EA-2) are similar for Pennsylvania and Wyoming angiosperms. Only one Wyoming conifer, *Juniperus osteosperma*, contained *n*-alkanes, and these had similar $\delta^{13}C$ *n*-alkane values to compounds in conifers from Pennsylvania. Bulk $\delta^{13}C$ values for the Wyoming conifers were significantly higher than for Pennsylvania (EA-2); the lower Δ_{leaf} values in Wyoming specimens are consistent with greater water stress. We omitted the lipid isotope data from statistical analyses for the *Juniperus osteosperma* because it is a single representative of its plant functional type in Wyoming. Isotopic fractionation during the biosynthesis of *n*-alkanes (relative to bulk leaf carbon) is expressed as ε values:

$$\varepsilon_{lipid} = \left[\frac{\delta^{13}C_{lipid} + 1000}{\delta^{13}C_{leaf} + 1000} - 1\right] \times 10^3 \approx (\delta^{13}C_{lipid} - \delta^{13}C_{leaf}) \quad (3)$$

following Chikaraishi et al. (2004). Both $\delta^{13}C$ and ε_{lipid} values decrease with increasing *n*-alkane chain lengths in the

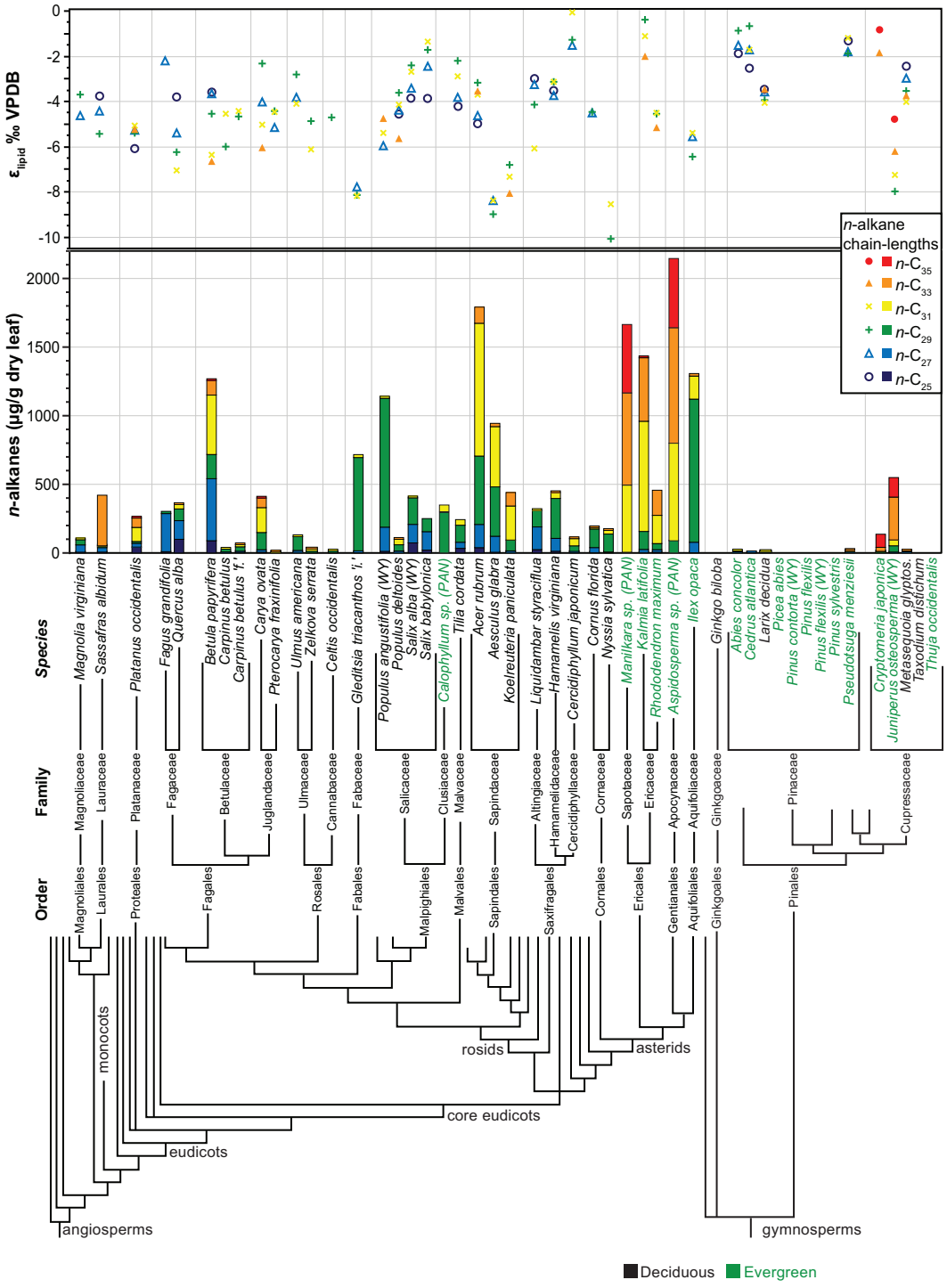

Fig. 2. Odd-chain *n*-alkane abundances (µg/g dry leaf) and ε_{lipid} values among leaves. Angiosperm phylogeny is constructed following The Angiosperm Phylogeny Group (2009) and gymnosperm phylogeny following Rai et al. (2008). Species from Wyoming (WY) and Panama (PAN) are denoted. The variation in total abundance and by chain length is higher for the angiosperms compared to the gymnosperms. Data is provided in Table 2, EA-1, and EA-2.

angiosperms (Fig. 8 and Table 3) and are similar between chain lengths in the gymnosperms. Angiosperm ε_{lipid} values are ~2‰ lower than in gymnosperms, with statistically significant differences between the two groups (Table 3) in *n*-C_{25} to *n*-C_{33}, except for *n*-C_{31} (marginally significant at $p = 0.06$).

4. DISCUSSION

4.1. *n*-Alkyl lipid abundances

Both *n*-alkane chain length distributions for *n*-C_{23} to *n*-C_{35} and CPI values are similar to those previously reported

Table 2
n-Alkane abundances (μg/g dry leaf) by plant functional type and phylogeny.

Chain length	DA[a]	EA	DG	EG	A	G	WRS (A vs G) [b]
n-C_{25}	18.9 ± 27.5	1.7 ± 2.2	0.8 ± 1.5	0.9 ± 1.7	15.7 ± 25.7	0.9 ± 1.6	$p<0.0001$
n-C_{27}	79.7 ± 104.4	20.4 ± 29.1	0.6 ± 1.1	1.7 ± 2.4	68.9 ± 97.6	1.4 ± 2.1	$p<0.0001$
n-C_{29}	162.4 ± 222.1	269.1 ± 389.5	1.6 ± 2.8	6.1 ± 13.6	181.8 ± 256.0	4.9 ± 11.8	$p<0.0001$
n-C_{31}	101.2 ± 210.9	405.1 ± 310.6	0.5 ± 0.8	4.2 ± 12.7	156.5 ± 255.7	3.2 ± 10.9	$p<0.0001$
n-C_{33}	32.4 ± 76.6	362.6 ± 351.5	0.0 ± 0.0	31 ± 93.7	92.4 ± 202.0	22.8 ± 80.4	$p=0.01$
n-C_{35}	0.3 ± 0.9	168.8 ± 257.6	0.0 ± 0.0	21.6 ± 49.3	30.9 ± 121.4	15.9 ± 42.8	ns

[a] Mean and standard deviation (1σ). Abbreviations are as follows: A, angiosperm; D, deciduous; E, evergreen; G, gymnosperm. Total number of species for each plant functional type is as follows: DA = 27, DG = 4, EA = 6, EG = 11, A = 33, G = 15.
[b] WRS, Wilcoxon rank-sum test (ns, not statistically different).

(Eglinton et al., 1962; Eglinton and Hamilton, 1967; Kolattukudy et al., 1976). However, the large variability in the total amount of *n*-alkanes (Figs. 2 and 3) has not been previously documented. Notably, *n*-alkane abundances differ significantly between the angiosperm and gymnosperm species, with the angiosperms having higher *n*-alkane abundances for each homologue between *n*-C_{25} and *n*-C_{31} (Table 2 and Fig. 3). In fact, many of the gymnosperm species investigated had no detectable *n*-alkanes (Fig. 2). The angiosperm–gymnosperm contrast accounts for the largest difference in *n*-alkane abundances, yet within these groups, they do not correlate with family. Further, abundances suggest leaf life-span is important. Among both angiosperms and gymnosperms, evergreens have higher *n*-alkane abundances than deciduous species for comparisons made between each chain-length from *n*-C_{29} to *n*-C_{35} (Fig. 3 and Table 2).

Differences in *n*-alkane production between phylogenetic groups are known to exist in modern and geologic samples. In leaves, leaf litter, and O-horizon of soils under angiosperm (*Populus tremula*) and conifer (*Pinus contorta*) forests (Otto and Simpson, 2005), *Populus tremula* leaves and soils contain high amounts of long-chain *n*-alkanes in contrast to *Pinus contorta* needles that had no detectable *n*-alkanes and soils contained low concentrations of *n*-alkanes (<40 μg/g carbon). The *n*-alkanes found in soils of the *Pinus contorta* forest likely come from small angiosperm shrubs and grasses, as supported by the presence of the angiosperm biomarkers α- and β-amyrin. Work by Otto and Simpson (2005) not only demonstrates that *n*-alkanes are preferentially produced by angiosperms, but it also shows that differences in plant wax production are transferred to soils. Phylogenetic differences in modern plants have also been observed in hydroxy fatty acids; Goñi and Hedges (1990) observed higher total cutin acids in gymnosperms compared to dicotyledonous angiosperms. Overall, we found total *n*-alkyl lipids are higher in angiosperms compared to gymnosperms (Fig. 4) and our data suggest gymnosperms maintain cuticle function with different biochemical compositions (e.g., greater hydroxy fatty acids, lower *n*-alkyl lipids) compared to angiosperms (e.g., lower hydroxy fatty acids, higher *n*-alkyl lipids).

In a study of Miocene conifer and angiosperm leaf fossils, Otto et al. (2003) identified *n*-alkanes in angiosperm genera but not in the conifers *Taxodium* and *Glyptostrobus*. They found minor amounts of *n*-C_{25} and *n*-C_{27} in *Calocedrus* sp. However, *n*-nonacosan-10-ol was very common in all conifer samples (Otto et al., 2003). This is also observed in modern plants, where morphologically distinct nonacosanol tubes are common on the surfaces of gymnosperms and rare on angiosperms leaves (Barthlott et al., 1998).

n-Alkane abundances are presented as mass of compound normalized to the dry mass of leaf material extracted. Yet, because *n*-alkanes are found within the cuticle and on the leaf surface (Eglinton et al., 1962; Eglinton and Hamilton, 1967), their abundances should scale with leaf surface area. The angiosperms in our study all have broad leaves whereas gymnosperms have needle leaves, except for *Gingko biloba*, which did not contain *n*-alkanes. Higher surface areas of the broad-leaf morphologies are not sufficient to account for the large *n*-alkane abundance difference between phylogenetic divisions. Although leaf mass per area (LMA) values for EGs are nearly twice that of DAs and EAs (Poorter et al., 2009), this does not explain the 100-fold higher *n*-alkane abundance in angiosperm leaves relative to gymnosperm needles.

LMA is correlated to leaf life-span in ecological studies (Wright et al., 2004) where longer leaf life-spans are associated with higher chemical construction costs (e.g., Williams et al., 1989; Villar and Merino, 2001). Therefore, it might be expected that lipid abundance will increase with LMA. However, neither total *n*-alkyl lipid nor total *n*-alkane abundance in this study is correlated with LMA (Fig. 5). This study confirms previous observations that total *n*-alkyl lipid abundance is not related to leaf life-span (Villar et al., 2006). Total wax content must be related to other factors that vary among plant groups such as evolutionary differences, growth strategies, plant physiology, etc. Further research is needed to clarify relationships between life-span length, leaf morphology and *n*-alkane production.

Early reports of average chain length suggested ACL is lower in cooler climates than warmer climates (Simoneit et al., 1977; Gagosian et al., 1987; Kvenvolden et al., 1987). In our study, ACL is highly variable, even within a phylogenic group or a PFT (Fig. 6 and EA-1), and the range is larger than in sedimentary archives (e.g., Smith et al., 2007). Our findings reinforce the idea (Collister et al., 1994) that sedimentary records of ACL can reflect change in community composition, although not in a simple or systematic way.

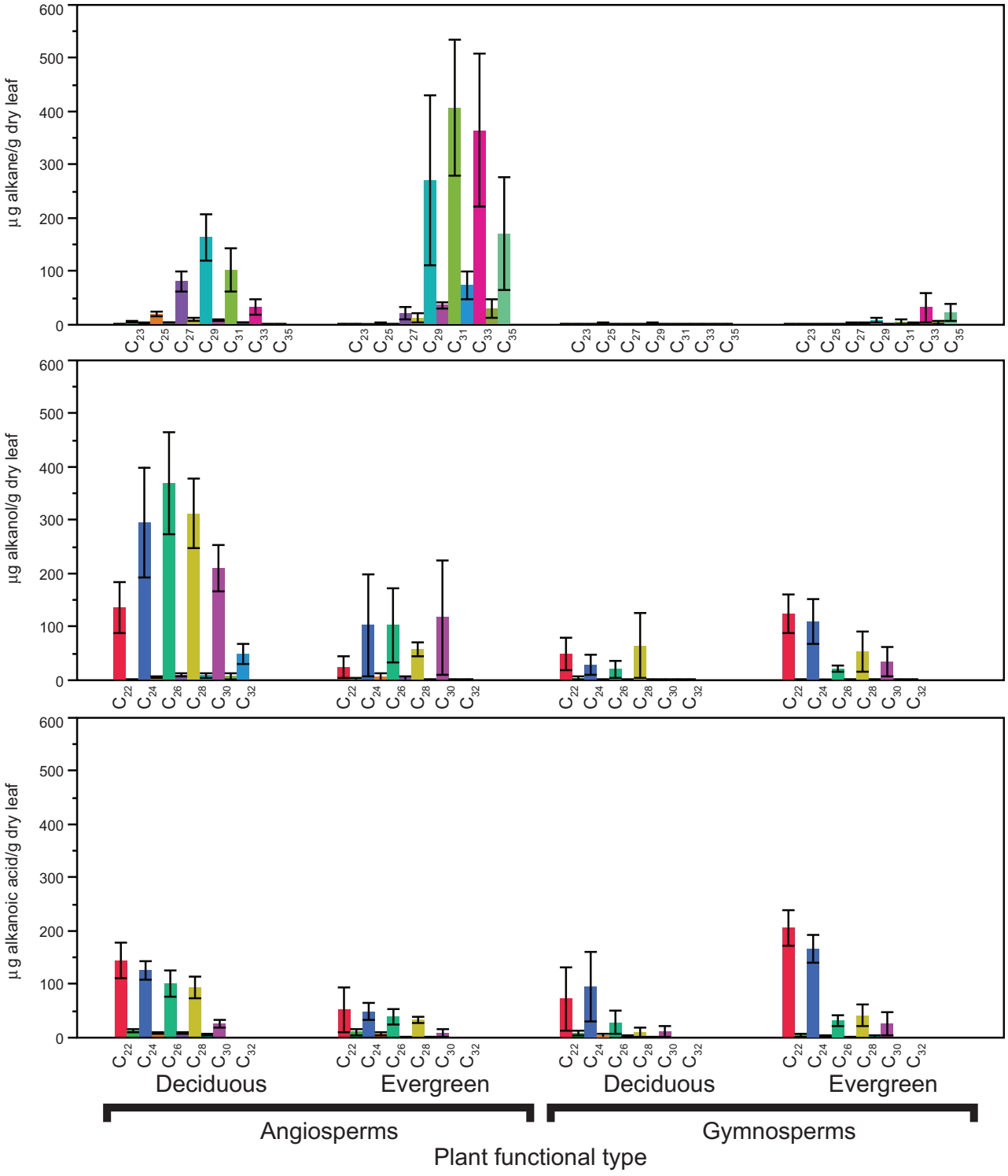

Fig. 3. Comparison of average *n*-alkane, *n*-alkanol, and *n*-alkanoic acid abundances (µg/g dry leaf) separated by chain length and plant functional type. Error bars denote standard error across all measurements for respective chain length. *n*-Alkane data is provided in Table 2 and EA-1.

4.2. *n*-Alkyl lipid biosynthetic fractionation patterns

We find a wide range in ε_{lipid} values (~10‰; Fig. 8) among angiosperms and a somewhat smaller range for conifer *n*-alkanes (~3‰). The range for angiosperm alkanes is much larger than for bulk $\delta^{13}C$ values (4‰). Mean values for ε_{lipid} between the major phylogenetic groups are statistically different (Fig. 8 and Table 3), with the angiosperms

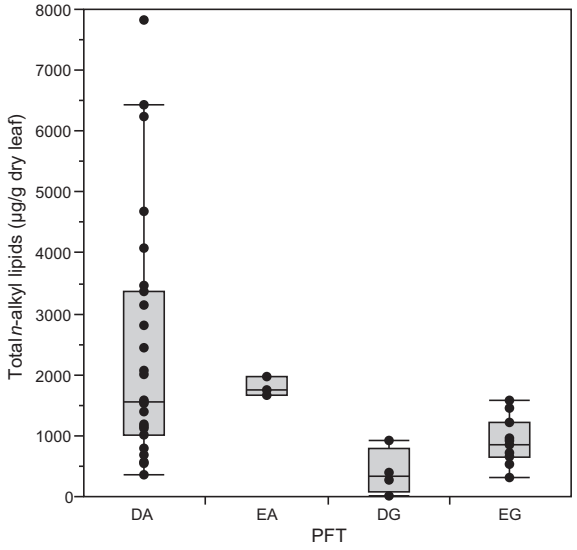

Fig. 4. Total *n*-alkyl lipid abundances including the *n*-alkanes (>*n*-C_{23}), *n*-alkanols (>*n*-C_{22}), and *n*-alkanoic acids (>*n*-C_{22}) separated by plant functional types (PFT) including deciduous angiosperms (DA), deciduous gymnosperms (DG), evergreen angiosperms (EA), and evergreen gymnosperms (DG).

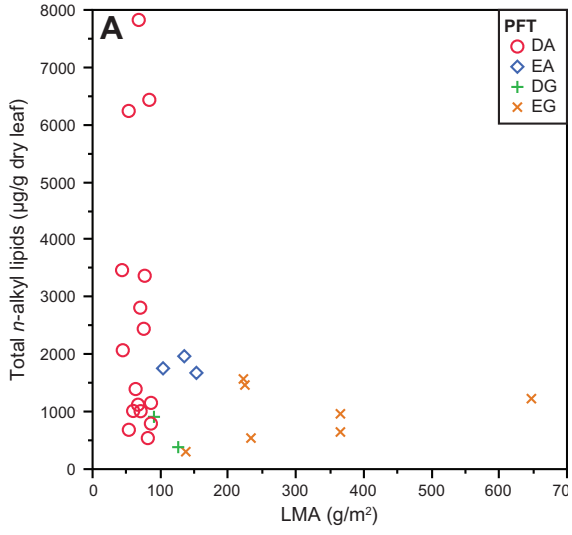

Fig. 5. Comparison of total *n*-alkyl lipid abundances (A) including the *n*-alkanes (>*n*-C_{23}), *n*-alkanols (>*n*-C_{22}), and *n*-alkanoic acids (>*n*-C_{22}) to leaf mass per area and comparison of total *n*-alkanes (B) to leaf mass per area. Samples are color-coded by plant functional type (PFT): deciduous angiosperms (DA), deciduous gymnosperms (DG), evergreen angiosperms (EA), and evergreen gymnosperms (DG). (For interpretation of the references to color in this figure legend, the reader is referred to the web version of this article.)

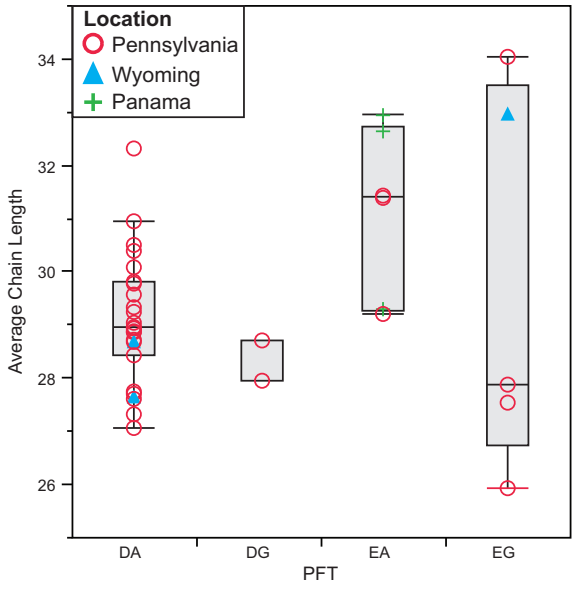

Fig. 6. Average chain length (ACL) separated by plant functional types (PFT) including deciduous angiosperms (DA), deciduous gymnosperms (DG), evergreen angiosperms (EA), and evergreen gymnosperms (DG). ACL data is provided in EA-1 and the number of samples within each PFT are as follows: DA = 27, DG = 2, EA = 6, EG = 5.

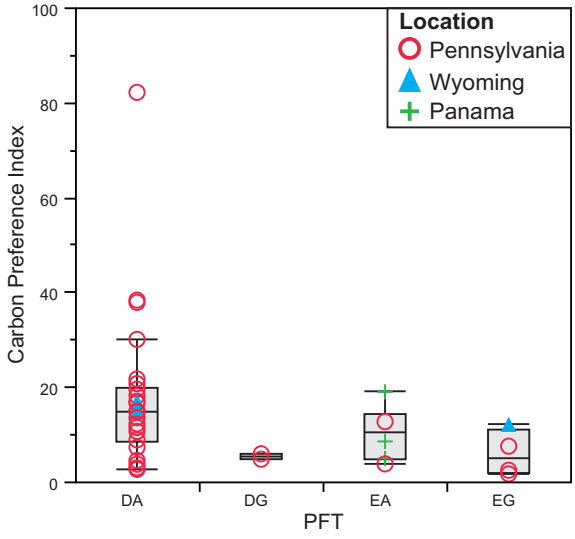

Fig. 7. Carbon preference index (CPI) separated by plant functional types (PFT) including deciduous angiosperms (DA), deciduous gymnosperms (DG), evergreen angiosperms (EA), and evergreen gymnosperms (DG). CPI data is provided in EA-1 and the number of samples within each PFT are as follows: DA = 26, DG = 2, EA = 6, EG = 4.

having mean ε_{lipid} values ~2‰ lower than the conifers. This wide range and the mean values are both similar to previous studies of temperate to subtropical angiosperms (Collister et al., 1994; Chikaraishi and Naraoka, 2003; Bi et al., 2005) and gymnosperms (Chikaraishi and Naraoka, 2003; Chikaraishi et al., 2004).

For plants grown in a similar environment, alkanes from gymnosperms will be ~4‰ enriched relative to those from angiosperms. This difference derives from the diminished Δ_{leaf} values (~2–3‰) documented for gymnosperms relative to angiosperms under similar climates (Pataki et al., 2003; Diefendorf et al., 2010) and ~2‰ higher mean ε_{lipid}

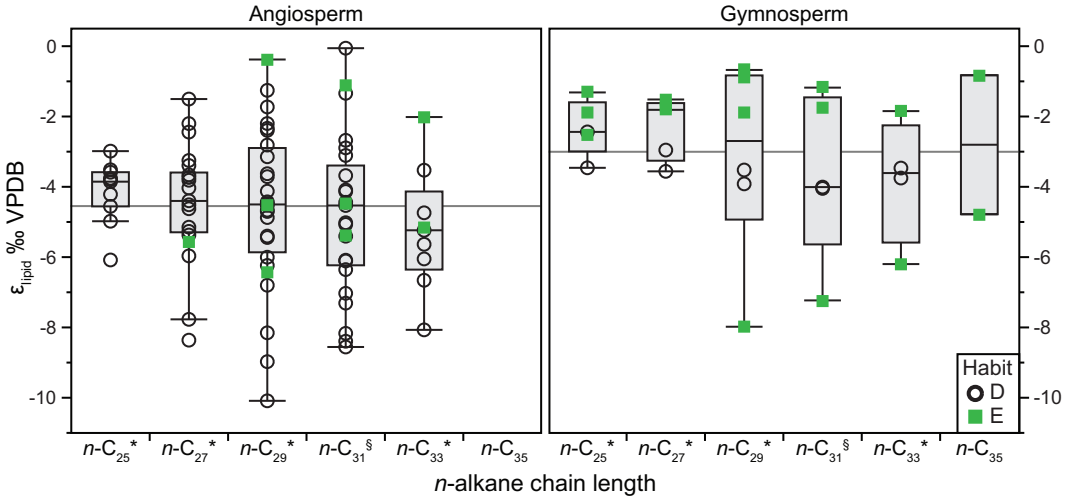

Fig. 8. Box and whisker plots for ε_{lipid} values separated by phylogeny and chain length. Box and whisker plots show the median, upper and lower quartiles, and maximum and minimum values, with outlier values noted. All values are provided in EA-2 and average data, standard deviations, number of samples, and statistical tests are provided in Table 3. Statistical comparisons between angiosperms and gymnosperms within a chain length are denoted next to each chain length within the figure for comparison (statistically significant at $p < 0.05$ or better, $*$; marginally significant at $p < 0.06$, §).

Table 3
ε_{lipid} comparisons by phylogeny and PFT.

ε_{lipid} *n*-alkane	DA[a]	DG	EA	EG	A	G	*t*-Test[b]
n-C_{23}	-3.2 ± 1.1 ($n = 5$)	-3.0 ($n = 1$)	na	-1.8 ± 1.3 ($n = 2$)	-3.2 ± 1.1 ($n = 5$)	-2.2 ± 1.1 ($n = 3$)	ns
n-C_{25}	-4.1 ± 0.8 ($n = 11$)	-3.0 ± 0.7 ($n = 2$)	na	-1.9 ± 0.6 ($n = 3$)	-4.1 ± 0.8 ($n = 11$)	-2.3 ± 0.8 ($n = 5$)	$p = 0.003$
n-C_{27}	-4.4 ± 1.6 ($n = 21$)	-3.3 ± 0.4 ($n = 2$)	-5.6 ($n = 1$)	-1.7 ± 0.2 ($n = 3$)	-4.5 ± 1.6 ($n = 22$)	-2.3 ± 0.9 ($n = 5$)	$p = 0.002$
n-C_{29}	-4.6 ± 2.2 ($n = 25$)	-3.7 ± 0.3 ($n = 2$)	-3.8 ± 3.1 ($n = 3$)	-1.2 ± 0.6 ($n = 3$)	-4.5 ± 2.3 ($n = 28$)	-2.2 ± 1.5 ($n = 5$)	$p = 0.019$
n-C_{31}	-5.0 ± 2.2 ($n = 22$)	-4.0 ± 0.0 ($n = 2$)	-3.7 ± 2.3 ($n = 3$)	-1.5 ± 0.4 ($n = 2$)	-4.8 ± 2.2 ($n = 25$)	-2.8 ± 1.5 ($n = 4$)	$p = 0.062$
n-C_{33}	-5.7 ± 1.4 ($n = 7$)	-3.6 ± 0.2 ($n = 2$)	-3.6 ± 2.2 ($n = 2$)	-1.9 ($n = 1$)	-5.3 ± 1.7 ($n = 9$)	-3.0 ± 1.0 ($n = 3$)	$p = 0.036$
n-C_{35}	na	na	na	na	na	na	ns

[a] Mean, standard deviation (1σ), and total specimens. Abbreviations are as follows: A, angiosperm; D, deciduous; E, evergreen; G, gymnosperm; na, not applicable.
[b] Statistical comparison between A and G. No statistical difference is denoted (ns).

values for the conifer lipids noted above. The difference from the combined influence of these factors is illustrated in Fig. 9, although we caution that this anticipated result is limited to temperate, C_3 tree leaves. We expect that lipid fractionation factors will be sensitive to influences on both the timing and carbon substrates involved in lipid synthesis, including seasonality, vegetational structure, climate conditions and plant types. For example, C_3 trees in savanna environments, which tend to be water-limited, have *n*-C_{31} alkane ε values that average -7 ± 2‰ (Vogts et al., 2009), while C_4 grasses in subtropical and warm temperate habitats ε values average -9.3 ± 2‰ (Krull et al., 2006; Rommerskirchen et al., 2006). Rainforest plants including C_3 trees have values that average ~-8‰ (Vogts et al., 2009). All of these tropical plant types exhibit significantly greater fractionation compared to our observations of -4.8 ± 2.2‰ for angiosperm trees in temperate environments (Table 3).

Differences between plant groups may reflect the timing of *n*-alkane production during the growing season (Pedentchouk et al., 2008) and/or allocation of carbon products derived from acetate (Hayes, 2001). Ontogenetic variation in *n*-alkane production within plants is complicated and presently not well described (Lockheart et al., 1997; Jetter and Schaffer, 2001; Samuels et al., 2008; Sachse et al., 2009). However, shifting fluxes of carbon within a cell to other biochemical fates (such as proteins and carbohydrates) can influence compound isotopic patterns (Hayes, 2001). Differing biochemical fluxes of pyruvate to fates other than acetyl-CoA via pyruvate dehydrogenase (for

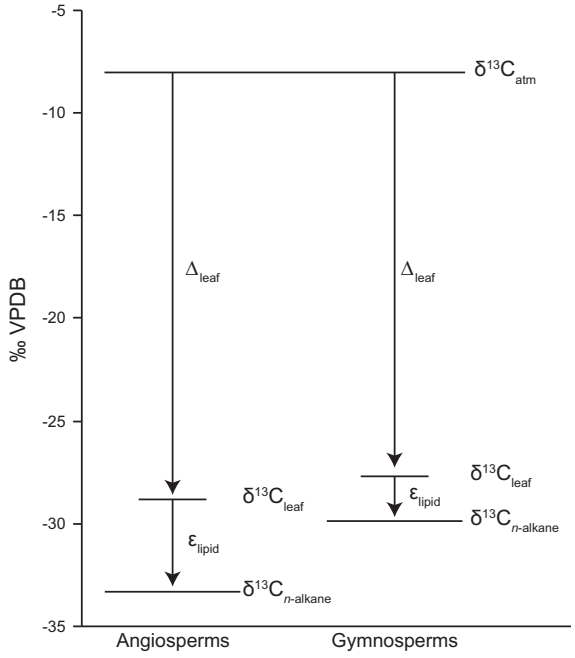

Fig. 9. Conceptual diagram of fractionation steps that occur from fixation of carbon during photosynthesis (Δ_{leaf}) and lipid biosynthesis (ε_{lipid}). $\delta^{13}C$ and ε values from n-C_{29} alkanes are averaged values for the angiosperm and gymnosperm species within this study (see Table 3). Angiosperms have higher ε_{lipid} and Δ_{leaf} values than gymnosperms (see Diefendorf et al., 2010) resulting in a much larger apparent fractionation between atmosphere and n-alkanes. This results in a $\delta^{13}C$ difference of at least 3‰ between phylogenetic groups.

example, to amino acid synthesis) can shift isotopic values of acetogenic lipids, with greater ^{13}C-depletion expected under decreased lipid production (Hayes, 2001). Thus, the overall greater discrimination for angiosperms is not consistent with their higher lipid abundances. Additionally, there is no correlation between ε_{lipid} values and n-alkyl lipid abundances. This is not surprising given that n-alkyl lipids typically comprise less than 0.1% of the total leaf mass. Alternatively, we suggest timing, seasonal variations, and changes in the sources or fates of pyruvate or acetyl-CoA during n-alkyl lipid synthesis most likely explain differences in ε_{lipid} observed here.

4.3. Implications for interpreting the geologic past

The higher production of n-alkanes in angiosperms compared to gymnosperms is documented in our study, in the modern forest example (Otto and Simpson, 2005), and the geologic example (Otto et al., 2003). These findings are significant given that many studies use n-alkanes for tracking $\delta^{13}C$ values of the atmosphere (see references in Pancost and Boot, 2004) and δD values of precipitation in the geologic past (e.g., Smith et al., 2007; Polissar et al., 2009). Further, angiosperms have different values for both ε_{lipid} (Fig. 8) and Δ_{leaf} compared to gymnosperms (see Diefendorf et al., 2010), which together result in $\delta^{13}C$ values of n-alkanes that are at least 4‰ lower in the angiosperms relative to gymnosperms.

Both fractionation and abundance differences between plant groups help us interpret $\delta^{13}C$ signatures of plant biomarkers from the geologic past. Forest leaf-litter production is similar for temperate forests with different plant functional types (Vogt et al., 1986). Because forest leaf-litter production is similar, the n-alkane signal preserved in soils and sediments will be dominated by the angiosperms in mixed angiosperm/gymnosperm forests. Therefore, unless leaf macrofossil or fossil cuticle data indicate a gymnosperm-dominated plant community, sedimentary n-alkanes are likely to be derived almost entirely from angiosperms.

At the transition from the Paleocene to Eocene, 55.8 million years ago, a large amount of carbon was added to the atmosphere, perturbing the global carbon cycle, and causing a period of rapid global warming (~5 °C; Wing et al., 2005). This event, the Paleocene–Eocene Thermal Maximum (PETM) is documented globally by a large negative carbon isotope excursion (CIE) (see Schouten et al., 2007). In the Bighorn Basin (WY, USA), the magnitude of the CIEs in terrestrial organic carbon and in atmospheric CO_2 likely differ because of changes in Δ_{leaf} that accompanied plant community shifts, warming, and decreased precipitation (Wing et al., 2005; Smith et al., 2007; Diefendorf et al., 2010). This plant community change, as documented from fossil leaf counts for major plant groups, indicates a change from a mixed angiosperm-conifer flora (~75% of leaf fossils counted are conifer) in the late Paleocene to an angiosperm flora (~100%) during the PETM. This change in plant community has been argued to result in an amplification of the CIE during the PETM due to the differences in Δ_{leaf} between angiosperms and conifers. Diefendorf et al. (2010) expanded this interpretation to correct Δ_{leaf} for the influence of both taxonomic change and concomitant changes in precipitation at the onset of the CIE. They estimated the CIE in atmospheric CO_2 to be 4.6‰ from $\delta^{13}C$ values of n-C_{31} alkanes in Smith et al. (2007). However, Diefendorf et al. (2010) made the assumption that angiosperms and conifers produce equal amounts of n-alkanes. If we consider the much higher production of n-alkanes by angiosperms, then the PETM plant CIE would reflect only the influence of precipitation, and we would estimate the CO_2 CIE to be ~5.6‰. If we assume that the flora during the PETM was dominated by DAs (this is unclear from fossil evidence, however DAs provide a more conservative n-alkane production estimate than EAs), and was a mix of DAs and DGs before and after the PETM (supported by the dominant *Metasequoia* and *Glyptostrobus* flora) (Wing et al., 2005), then there is almost a 200-fold difference in production between DAs (101 μg/g) and DGs (0.5 μg/g) for the n-C_{31} alkanes. Therefore, even if the plant community were 90% conifer prior to the PETM (not supported by fossil evidence), the angiosperms would still produce 95% of the n-alkanes. It is important to note that a nearly complete change in the angiosperm species across the PETM (Wing et al., 2005) may also have affected the size of the CIE because of differences in Δ_{leaf} and in ε_{lipid} among species (Diefendorf et al., 2010).

The PETM recorded in arctic sediments also captures a CIE that is larger than the marine record. However, the magnitudes of plant CIE values vary with n-alkane chain-

length (Pagani et al., 2006; Schouten et al., 2007). For example, the plant lipid CIE is ~6‰ in the *n*-C_{27} alkane (Pagani et al., 2006) and ~4.5‰ in the *n*-C_{29} alkane (Pagani et al., 2006; Schouten et al., 2007). It is unclear why the CIE is smaller in the *n*-C_{29} alkane compared to the *n*-C_{27} alkane and it has been suggested to reflect mixing between angiosperm and gymnosperm derived *n*-alkanes (Schouten et al., 2007); the CIE in gymnosperms is 3‰ based on tricyclic diterpenoids specific for gymnosperms and 6‰ based on pentacyclic triterpenoid biomarkers specific for angiosperm floras (Schouten et al., 2007). Given the *n*-alkane production bias by angiosperms shown here and the greater percentage of angiosperm floras in the arctic during the PETM (Schouten et al., 2007), we suggest the *n*-alkane CIE likely reflects only angiosperm inputs. PETM CIEs also vary between *n*-alkane chain-lengths at other sites including the Bighorn Basin in Wyoming (Smith et al., 2007) and in Tanzania (Handley et al., 2008). These differences in CIEs among *n*-alkane chain-lengths could be caused by changes in angiosperm species composition during the PETM, given that average chain-length, Δ_{leaf}, and $\varepsilon_{n\text{-alkane}}$ values vary between species. Plant biomarker CIEs are all large, between 4.5‰ and 6‰, and are similar to results for various proxies and locations (see compilation in Schouten et al., 2007 and McInerney and Wing, 2011). If the atmospheric CO_2 CIE was as large as 5–6‰ as suggested here, a greater mass of carbon and/or more ^{13}C depleted carbon would be required to explain the CIE. Although we have refined the interpretation of $\delta^{13}C$ values of *n*-alkanes by recognizing their angiosperm source, future research must address differences in CIEs between *n*-alkane chain-lengths by examining the timing of *n*-alkane synthesis and potential climate effects on $\varepsilon_{n\text{-alkanes}}$ between chain-lengths.

5. CONCLUSIONS

The abundances of *n*-alkanes of different chain-lengths, although variable, show consistent differences between two major plant groups. Of the gymnosperm species investigated here, nearly half did not produce *n*-alkanes, and angiosperms produce significantly higher concentrations of *n*-alkanes than gymnosperms in general. Although our study is limited to two sites and does not take into account the effects of climate, altitude, ontogeny, and other important factors, similar observations have been made in soils and fossils (Otto et al., 2003; Otto and Simpson, 2005).

Our results also indicate that biosynthetic carbon isotope fractionation during the production of *n*-alkanes, although variable among angiosperms, is ~2‰ greater than for the gymnosperms. These differences in fractionation and production of *n*-alkanes help refine our interpretation of plant signatures in the geologic record. We argue that the *n*-alkane biomarker record will largely (but not exclusively) represent angiosperms if both groups are present. Gymnosperm-derived *n*-alkanes may be significant in some assemblages and independent fossil data will be essential to discern the relative importance of gymnosperm-derived *n*-alkanes. Constraining ε_{lipid} differences between taxonomic groups further refines biomarker-based estimates of plant biomass $\delta^{13}C$ values. By incorporating ε_{lipid} differences, information about plant communities and models for Δ_{leaf} (Diefendorf et al., 2010), we can strengthen future reconstructions of the terrestrial carbon cycle over Earth history.

ACKNOWLEDGMENTS

We thank Laurie Eccles for laboratory preparation, Kevin Mueller and Emily Diefendorf for sample collection assistance, and Denny Walizer for technical support. We also thank two anonymous reviewers, Rienk Smittenberg and Associate Editor Josef Werne for their helpful suggestions. This research was supported by the National Science Foundation Grant EAR-0844212 (to K.H.F.) and fellowship awards from the Penn State Biogeochemical Research Initiative for Education (BRIE) funded by the National Science Foundation Integrative Graduate Education and Research Traineeship (IGERT Grant DGE-9972759).

APPENDIX A. SUPPLEMENTARY DATA

Supplementary data associated with this article can be found, in the online version, at doi:10.1016/j.gca.2011.09.028.

REFERENCES

Baker E. (1982) Chemistry and morphology of plant epicuticular waxes. In *The Plant Cuticle. Linnean Society Symposium Series* (eds. D. Cutler, K. Alvin and C. Price). Academic Press, London, pp. 139–165.

Bargel H., Koch K., Cerman Z. and Neinhuis C. (2006) Structure–function relationships of the plant cuticle and cuticular waxes – a smart material? *Funct. Plant Bio.* **33**, 893–910.

Barthlott W., Neinhuis C., Cutler D., Ditsch F., Meusel I., Theisen I. and Wilhelmi H. (1998) Classification and terminology of plant epicuticular waxes. *Bot. J. Linnean Soc.* **126**, 237–260.

Bi X., Sheng G., Liu X., Li C. and Fu J. (2005) Molecular and carbon and hydrogen isotopic composition of *n*-alkanes in plant leaf waxes. *Org. Geochem.* **36**, 1405–1417.

Bird M. I., Summons R. E., Gagan M. K., Roksandic Z., Dowling L., Head J., Keith Fifield L., Cresswell R. G. and Johnson D. P. (1995) Terrestrial vegetation change inferred from *n*-alkane $\delta^{13}C$ analysis in the marine environment. *Geochim. Cosmochim. Acta* **59**, 2853–2857.

Bray E. E. and Evans E. D. (1961) Distribution of *n*-paraffins as a clue to recognition of source beds. *Geochim. Cosmochim. Acta* **22**, 2–15.

Chikaraishi Y. and Naraoka H. (2003) Compound-specific δD–$\delta^{13}C$ analyses of *n*-alkanes extracted from terrestrial and aquatic plants. *Phytochemistry* **63**, 361–371.

Chikaraishi Y., Naraoka H. and Poulson S. R. (2004) Carbon and hydrogen isotopic fractionation during lipid biosynthesis in a higher plant (*Cryptomeria japonica*). *Phytochemistry* **65**, 323–330.

Collister J. W., Rieley G., Stern B., Eglinton G. and Fry B. (1994) Compound-specific $\delta^{13}C$ analyses of leaf lipids from plants with differing carbon dioxide metabolisms. *Org. Geochem.* **21**, 619–627.

Coplen T. B., Brand W. A., Gehre M., Groning M., Meijer H. A. J., Toman B. and Verkouteren R. M. (2006) New guidelines for $\delta^{13}C$ measurements. *Anal. Chem.* **78**, 2439–2441.

Cranwell P. A. (1981) Diagenesis of free and bound lipids in terrestrial detritus deposited in a lacustrine sediment. *Org. Geochem.* **3**, 79–89.

Deines P. (1980) The isotopic composition of reduced organic carbon. In *Handbook of Environmental Isotope Geochemistry* (eds. P. Fritz and J. C. Fontes). Elsevier, Amsterdam, pp. 329–406.

Diefendorf A. F., Mueller K. E., Wing S. L., Koch P. L. and Freeman K. H. (2010) Global patterns in leaf ^{13}C discrimination and implications for studies of past and future climate. *Proc. Natl. Acad. Sci.* **107**, 5738–5743.

Dodd R. S. and Poveda M. M. (2003) Environmental gradients and population divergence contribute to variation in cuticular wax composition in *Juniperus communis*. *Biochem. Syst. Ecol.* **31**, 1257–1270.

Eglinton G., Gonzalez A. G., Hamilton R. J. and Raphael R. A. (1962) Hydrocarbon constituents of the wax coatings of plant leaves: a taxonomic survey. *Phytochemistry* **1**, 89–102.

Eglinton G. and Hamilton R. J. (1967) Leaf epicuticular waxes. *Science* **156**, 1322–1335.

Farquhar G. D., Ehleringer J. R. and Hubick K. T. (1989) Carbon isotope discrimination and photosynthesis. *Annu. Rev. Plant Phys. Plant Biol.* **40**, 503–537.

Freeman K. H. and Colarusso L. A. (2001) Molecular and isotopic records of C4 grassland expansion in the late Miocene. *Geochim. Cosmochim. Acta* **65**, 1439–1454.

Freeman K. H. and Hayes J. M. (1992) Fractionation of carbon isotopes by phytoplankton and estimates of ancient CO_2 levels. *Global Biogeochem. Cycles* **6**, 185–198.

Gagosian R. B., Peltzer E. T. and Merrill J. T. (1987) Long-range transport of terrestrially derived lipids in aerosols from the south-Pacific. *Nature* **325**, 800–804.

Goñi M. A. and Hedges J. I. (1990) Cutin-derived CuO reaction products from purified cuticles and tree leaves. *Geochim. Cosmochim. Acta* **54**, 3065–3072.

Handley L., Pearson P. N., McMillan I. K. and Pancost R. D. (2008) Large terrestrial and marine carbon and hydrogen isotope excursions in a new Paleocene/Eocene boundary section from Tanzania. *Earth Planet Sci. Lett.* **275**, 17–25.

Hayes J. M. (2001) Fractionation of carbon and hydrogen isotopes in biosynthetic processes. *Rev. Mineral. Geochem.* **43**, 225–277.

Holloway P. H. and Williams F. L. (1982) Stability of carbon islands on 90% Rh–10% Pt (1 1 1) surfaces. *Appl. Surf. Sci.* **10**, 1–9.

Huang Y., Lockheart M. J., Collister J. W. and Eglinton G. (1995) Molecular and isotopic biogeochemistry of the Miocene Clarkia Formation: hydrocarbons and alcohols. *Org. Geochem.* **23**, 785–801.

Jetter R. and Schaffer S. (2001) Chemical composition of the *Prunus laurocerasus* leaf surface. Dynamic changes of the epicuticular wax film during leaf development. *Plant Physiol.* **126**, 1725–1737.

Jetter R., Schaffer S. and Riederer M. (2000) Leaf cuticular waxes are arranged in chemically and mechanically distinct layers: evidence from *Prunus laurocerasus* L. *Plant Cell Environ.* **23**, 619–628.

Koch K. and Ensikat H. J. (2008) The hydrophobic coatings of plant surfaces: epicuticular wax crystals and their morphologies, crystallinity and molecular self-assembly. *Micron* **39**, 759–772.

Kolattukudy P. (1996) Biosynthetic pathways of cutin and waxes, their sensitivity to environmental stresses. In *Plant Cuticles. An Integrated Functional Approach* (ed. G. Kersteins). BIOS Scientific Publishers Ltd., Oxford, pp. 83–108.

Kolattukudy P., Croteau R. and Buckner J. (1976) Biochemistry of plant waxes. In *Chemistry and Biochemistry of Natural Waxes* (ed. P. Kolattukudy). Elsevier, Amsterdam, pp. 289–347.

Krull E., Sachse D., Mügler I., Thiele A. and Gleixner G. (2006) Compound-specific δC and δH analyses of plant and soil organic matter: a preliminary assessment of the effects of vegetation change on ecosystem hydrology. *Soil Biol. Biochem.* **38**, 3211–3221.

Kunst L. and Samuels A. L. (2003) Biosynthesis and secretion of plant cuticular wax. *Prog. Lipid Res.* **42**, 51–80.

Kvenvolden K. A., Rapp J. B., Golanbac M. and Hostettler F. D. (1987) Multiple sources of alkanes in Quaternary oceanic sediment of Antarctica. *Org. Geochem.* **11**, 291–302.

Lockheart M. J., Van Bergen P. F. and Evershed R. P. (1997) Variations in the stable carbon isotope compositions of individual lipids from the leaves of modern angiosperms: implications for the study of higher land plant-derived sedimentary organic matter. *Org. Geochem.* **26**, 137–153.

Logan G. A., Smiley C. J. and Eglinton G. (1995) Preservation of fossil leaf waxes in association with their source tissues, Clarkia, northern Idaho, USA. *Geochim. Cosmochim. Acta* **59**, 751–763.

McInerney F. A. and Wing S. L. (2011) The Paleocene-Eocene Thermal Maximum: a perturbation of carbon cycle, climate, and biosphere with implications for the future. *Annu. Rev. Earth Planet Sci.* **39**, 489–516.

Muller C. and Riederer M. (2005) Plant surface properties in chemical ecology. *J. Chem. Ecol.* **31**, 2621–2651.

Otto A., Simoneit B. R. T. and Rember W. C. (2003) Resin compounds from the seed cones of three fossil conifer species from the Miocene Clarkia flora, Emerald Creek, Idaho, USA, and from related extant species. *Rev. Palaeobot. Palynol.* **126**, 225–241.

Otto A. and Simpson M. J. (2005) Degradation and preservation of vascular plant-derived biomarkers in grassland and forest soils from western Canada. *Biogeochemistry* **74**, 377.

Pagani M., Pedentchouk N., Huber M., Sluijs A., Schouten S., Brinkhuis H., Sinninghe Damste J. S., Dickens G. R. and Scienctists T. E. (2006) Arctic hydrology during global warming at the Palaeocene/Eocene thermal maximum. *Nature* **442**, 671–675.

Pancost R. D. and Boot C. S. (2004) The palaeoclimatic utility of terrestrial biomarkers in marine sediments. *Mar. Chem.* **92**, 239–261.

Pataki D. E., Ehleringer J. R., Flanagan L. B., Yakir D., Bowling D. R., Still C. J., Buchmann N., Kaplan J. O. and Berry J. A. (2003) The application and interpretation of Keeling plots in terrestrial carbon cycle research. *Global Biogeochem. Cycles* **17**, 1022.

Pedentchouk N., Sumner W., Tipple B. and Pagani M. (2008) $\delta^{13}C$ and δD compositions of *n*-alkanes from modern angiosperms and conifers: an experimental set up in central Washington State, USA. *Org. Geochem.* **39**, 1066–1071.

Piasentier E., Bovolenta S. and Malossini F. (2000) The *n*-alkane concentrations in buds and leaves of browsed broadleaf trees. *J. Agric. Sci.* **135**, 311–320.

Polissar P. J., Freeman K. H., Rowley D. B., McInerney F. A. and Currie B. S. (2009) Paleoaltimetry of the Tibetan Plateau from D/H ratios of lipid biomarkers. *Earth Planet Sci. Lett.* **287**, 64–76.

Poorter H., Niinemets U., Poorter L., Wright I. J. and Villar R. (2009) Causes and consequences of variation in leaf mass per area (LMA): a meta-analysis. *New Phytol.* **182**, 565–588.

Primack R. B. and Miller-Rushing A. J. (2009) The role of botanical gardens in climate change research. *New Phytol.* **182**, 303–313.

Rai H. S., Reeves P. A., Peakall R., Olmstead R. G. and Graham S. W. (2008) Inference of higher-order conifer relationships from a multi-locus plastid data set. *Botany* **86**, 658–669.

Riederer M. and Schreiber L. (2001) Protecting against water loss: analysis of the barrier properties of plant cuticles. *J. Exp. Bot.* **52**, 2023–2032.

Roderick M. L. and Cochrane M. J. (2002) On the conservative nature of the leaf mass–area relationship. *Ann. Bot.* **89**, 537–542.

Rommerskirchen F., Plader A., Eglinton G., Chikaraishi Y. and Rullkötter J. R. (2006) Chemotaxonomic significance of distribution and stable carbon isotopic composition of long-chain alkanes and alkan-1-ols in C4 grass waxes. *Org. Geochem.* **37**, 1303–1332.

Sachse D., Kahmen A. and Gleixner G. (2009) Significant seasonal variation in the hydrogen isotopic composition of leaf-wax lipids for two deciduous tree ecosystems (*Fagus sylvativa* and *Acer pseudoplatanus*). *Org. Geochem.* **40**, 732–742.

Samuels L., Kunst L. and Jetter R. (2008) Sealing plant surfaces: cuticular wax formation by epidermal cells. *Ann. Rev. Plant Biol.* **59**, 683–707.

Schouten S., Woltering M., Rijpstra W. I. C., Sluijs A., Brinkhuis H. and Sinninghe Damste J. S. (2007) The Paleocene–Eocene carbon isotope excursion in higher plant organic matter: differential fractionation of angiosperms and conifers in the Arctic. *Earth Planet Sci. Lett.* **258**, 581–592.

Sessions A. L. (2006) Seasonal changes in D/H fractionation accompanying lipid biosynthesis in *Spartina alterniflora*. *Geochim. Cosmochim. Acta* **70**, 2153–2162.

Shepherd T. and Griffiths D. W. (2006) The effects of stress on plant cuticular waxes. *New Phytol.* **171**, 469–499.

Simoneit B. R. T., Chester R. and Eglinton G. (1977) Biogenic lipids in particulates from lower atmosphere over eastern Atlantic. *Nature* **267**, 682–685.

Smith F. A., Wing S. L. and Freeman K. H. (2007) Carbon and hydrogen isotope compositions of plant lipids during the PETM as evidence for the response of terrestrial ecosystems to rapid climate change. *Earth Planet Sci. Lett.* **262**, 50–65.

The Angiosperm Phylogeny Group (2009) An update of the Angiosperm Phylogeny Group classification for the orders and families of flowering plants: APG III. *Bot. J. Linnean Soc.* **161**, 105–121.

Villar R. and Merino J. (2001) Comparison of leaf construction costs in woody species with differing leaf life-spans in contrasting ecosystems. *New Phytol.* **151**, 213–226.

Villar R., Robleto J. R., De Jong Y. and Poorter H. (2006) Differences in construction costs and chemical composition between deciduous and evergreen woody species are small as compared to differences among families. *Plant Cell Environ.* **29**, 1629–1643.

Vogt K. A., Grier C. C. and Vogt D. J. (1986) Production, turnover, and nutrient dynamics of aboveground and belowground detritus of world forests. *Adv. Ecol. Res.* **15**, 303–377.

Vogts A., Moossen H., Rommerskirchen F. and Rullkötter J. R. (2009) Distribution patterns and stable carbon isotopic composition of alkanes and alkan-1-ols from plant waxes of African rain forest and savanna C3 species. *Org. Geochem.* **40**, 1037–1054.

Williams K., Field C. B. and Mooney H. A. (1989) Relationships among leaf construction cost, leaf longevity, and light environment in rain-forest plants of the genus *Piper*. *Am. Nat.* **133**, 198–211.

Wing S. L., Harrington G. J., Smith F. A., Bloch J. I., Boyer D. M. and Freeman K. H. (2005) Transient floral change and rapid global warming at the Paleocene–Eocene boundary. *Science* **310**, 993–996.

Wright I. J., Reich P. B., Westoby M., Ackerly D. D., Baruch Z., Bongers F., Cavender-Bares J., Chapin T., Cornelissen J. H. C., Diemer M., Flexas J., Garnier E., Groom P. K., Gulias J., Hikosaka K., Lamont B. B., Lee T., Lee W., Lusk C., Midgley J. J., Navas M.-L., Niinemets U., Oleksyn J., Osada N., Poorter H., Poot P., Prior L., Pyankov V. I., Roumet C., Thomas S. C., Tjoelker M. G., Veneklaas E. J. and Villar R. (2004) The worldwide leaf economics spectrum. *Nature* **428**, 821–827.

Associate editor: Josef Werne